Journal of Soil Science and Plant Nutrition (2022) 22:3334–3347
https://doi.org/10.1007/s42729-022-00890-0

ORIGINAL PAPER

# Does Structural Equation Modeling Provide a Holistic View of Phosphorus Acquisition Strategies in Soils of Amazon Forest?

Erika Caitano da Silva[1] · Marcus Vinicius da Silva Sales[2] · Seldon Aleixo[3] · Antonio Carlos Gama-Rodrigues[1] · Emanuela Forestieri Gama-Rodrigues[1]

Received: 24 September 2021 / Accepted: 25 May 2022 / Published online: 6 June 2022

## Abstract

The development and productivity of the Amazon Forest are limited by the availability of phosphorus (P) in P-impoverished soils. Applying structural equation modeling (SEM) to develop hypothetical models capable of integrating multiple P absorption strategies and its soil cycle enables holistic understanding of the functionality of tropical forest ecosystems. Six structural models were developed using latent variables and their respective measurable indicators, and grouped into soil P pool ($P_o$, $P_i$, occluded P), pools of root morphology (specific root length, root tissue density, and mean root diameter), biotic absorption (arbuscular mycorrhizal associations), and physiological absorption (acidic root phosphomonoesterase enzyme). All structural models confirm the theoretical concept of interdependence between P pools and pools with different P absorption strategies used by the Amazon Forest in P-impoverished soils. The models demonstrated that root morphology has a significant and simultaneous influence on mycorrhizal fungi and acid phosphomonoesterase activity, and that $P_o$ is the main source of P for maintaining the forest ecosystem. Structural equation modeling with latent variables was able to simplify the relationship between the P cycle and plant strategies for P acquisition, and thus provide a holistic view of these mechanisms in low fertility soils in Central Amazonia. The models showed that all P uptake strategies manifest themselves simultaneously at the ecosystem level, but the predominance of a given strategy will depend on the metabolic cost/benefit balance as a function of P transformations in the soil of the forest site.

**Keywords** Organic P · P absorption strategies · Structural models · Amazon Forest

## Abbreviations

| | |
|---|---|
| SEM | Structural equation modeling |
| SRL | Specific root length |
| SRA | Specific root area |
| RTD | Root tissue density |
| MRD | Mean root diameter |
| AM | Arbuscular mycorrhizas |
| APase | Acid phosphomonoesterase |
| $P_i$ | Inorganic phosphorus |
| $P_o$ | Organic phosphorus |

## 1 Introduction

The tropical forests of the Amazon Basin occur on a wide variety of different soil orders reflecting a rich diversity of geologic origins and geomorphic processes (Quesada et al. 2011), with about 30% represented by oxisols (Malhi and Wright 2004; Quesada et al. 2011). These soil orders are characterized as severely phosphorus-impoverished soils because they release a small fraction of phosphorus (P) by the weathering of parent material, and have high P sorption capacity (de Mesquita Filho and Torrent 1993; Driessen et al. 2001; Quesada et al. 2011). Readily available mineral P ($P_i$) decreases during pedogenesis, and most P is in organic forms ($P_o$) or bound to soil minerals or occluded within Al and Fe oxides (Walker and Syers 1976). Thus, at a later stage of pedogenesis, $P_o$ becomes the main pool of P for

✉ Antonio Carlos Gama-Rodrigues
tonygama@uenf.br

[1] Universidade Estadual do Norte Fluminense Darcy Ribeiro - UENF/CCTA/Laboratório de Solos, Av. Alberto Lamego 2000, Campos dos Goytacazes, RJ CEP 28013-602, Brazil

[2] Departamento de Ciências Econômicas de Campos, Universidade Federal Fluminense - UFF, Campos dos Goytacazes, RJ, Brazil

[3] Laboratório de Ciências Químicas - UENF, Campos dos Goytacazes, RJ, Brazil

the maintenance of forest ecosystems (Turner and Condron, 2013). $P_o$ inputs into the soil occur by the roots, litter, and microbial biomass (Bünemann and Condron 2007; Condron et al. 2005; George et al. 2018; Rubaek and Sibbesen 1993).

In this sense, it is important to understand how tropical forests manage to maintain plant growth and production, even with restricted soil P availability. Tropical tree species have adapted and evolved several root strategies to enhance $P_i$ acquisition in low-P environments (Guilbeault-Mayers et al. 2020; Reichert et al. 2022), including root architecture and morphology related to improving P-uptake (Freschet et al. 2021; Haling et al. 2018; Postma et al. 2014; Vance et al. 2003); synthesis of root phosphatase enzymes, secretion of organic anions, and release of protons in the rhizosphere region increasing mobilization of moderately labile $P_i$ and $P_o$ (Han et al. 2021; Hinsinger et al. 2003; Pang et al. 2018; Richardson and Simpson 2011); and symbiotic associations with arbuscular mycorrhizal (AM) fungi, in which hyphae can access labile $P_i$ and exploit soil micropores that the root system cannot reach (Clark and Zeto 2000; Reichert et al. 2022; Smith et al. 2011; van der Heijden et al. 2015); AM fungi are also able to synthesize phosphatase enzymes to access organic sources of P that are not initially available to plants (Liu et al. 2018; Turner, 2008).

In a recent study, Lugli et al. (2020) aimed to understand the P acquisition strategies in a forest site in the Central Amazon region by evaluating the morphological, physiological (phosphatase activities — *APase*), and biotic (arbuscular mycorrhizal associations — AM) adaptations of the rhizosphere. Using bivariate correlations, these authors reported that root morphology would be the main mechanism to increase the P uptake efficiency in the soil, while $P_i$ uptake by AM and $P_o$ hydrolysis by *APase* enzyme exudation were considered complementary mechanisms for acquiring the element. However, as the bivariate correlations do not integrate the different relationships which influence the functional characteristics of the roots, they do not provide a holistic view of the different strategies that can be used by the root system to increase the obtainment of P in the soil.

The holistic approach of P acquisition strategies requires the use of statistical techniques which enable a multivariate overview of the soil–plant system so that hypotheses can be developed from solid foundations. In this sense, the use of structural equation modeling (SEM) with latent variables combined with the use of P fractionation techniques has provided important contributions to the understanding of the P cycle, in which the organic P pool constitutes the main source to the available P pool in highly weathered tropical forest soils (Costa et al. 2016; Gama-Rodrigues et al. 2014; Sales et al. 2017; Viana et al. 2018). However, none of these studies addressed root system traits related to P uptake. Therefore, the use of SEM to deepen these studies is a novelty that can collaborate to confirm concepts in more detail or reveal hypotheses that will help to understand the functioning of natural ecosystems and enable their sustainable management.

Structural equation modeling (SEM) is being increasingly used in confirmatory multivariate tests or in exploring possible alternative hypotheses in natural systems (Grace et al. 2010). The ability to perform confirmatory tests and testing multivariate hypothesis allows SEM to move beyond the descriptive nature of traditional statistics to a more advanced inferential approach (Grace and Bollen, 2006). Simplifying and integrating factors that can influence the transformations of a given ecosystem is possible by joining measurable variables with latent variables (constructs) in a hypothetical model (Grace and Bollen 2006; Oliveira et al. 2018). Latent variables are not measured, and therefore, they are conceptualized through the theory on a given topic; thus, it is possible to represent underlying causes that can increase understanding of the interconnections related to the soil–plant system (Rinaldi et al. 2021). Another advantage of using the constructs is the approach to measurement errors, which can happen during data collection, but which are not considered in conventional statistical analyses. Both the use of error variances and the addition of a covariation relation enable discovering external influences which were not considered in the hypothetical model, but that may be inducing the fitted structural model (Grace et al 2014; Hair et al. 2009).

The hypothesis of the present study is that hypothetical structural models capable of integrating the soil P cycle and the multiple P acquisition strategies by plants allow a holistic understanding of the functionality of tropical forest ecosystems. To address this, we used the SEM method with latent variables to demonstrate the interconnections that occur between the different morphological, physiological, and biotic adaptations of the rhizosphere and the different soil P forms in P-impoverished environments in Central Amazonia.

## 2 Material and Methods

### 2.1 Data Collection

Structural models were built with data from Lugli et al. (2020) collected from oxisols under an ancient *terra firme* lowland forest with a mean annual rainfall of 2400 mm, no water deficit, and mean annual temperature of 26 °C, located in the municipality of Manaus, State of Amazonas, Brazil. The study related P fractionation with some plant strategies for uptake in soils with low P levels in a Central Amazon forest. Hedley fractionation (Hedley et al., 1982) was used to obtain fractions (mg $kg^{-1}$) of organic P ($P_o$), inorganic P ($P_i$), and occluded P for the 0–10-cm soil depth from 32 plots (40 m × 40 m) established in areas with similar soil, vegetation (high species diversity), and flat relief, with plots at least 50 m away from each other. Total P (acid digestion) ranged from 118 to 217 mg kg$^{-1}$, while the fractions of Resin-P ranged from 2.6 to 6.4, bicarbonate-P$_i$ varied from 0.4 to 2.5, bicarbonate-P$_o$ ranged from 3.7 to 10.1, hydroxide-P$_i$ varied from 11.3 to 20.7, hydroxide-P$_o$ ranged from 9.7 to 19.1, HCl-P varied from 0.8 to 2.3, and residual P ranged from 69 to 167 mg kg$^{-1}$. Root morphology data of different individuals from the forest site were used to represent the different P uptake strategies, with measurements of mean root diameter (MRD: 0.39–1.11 mm), specific root length (SRL: 0.59–4.15 cm mg$^{-1}$), and root tissue density (RTD: 142–419 mg cm$^{-3}$). Data on the root acid phosphomonoesterase enzyme activity (*APase*: 16–66 nmol mg$^{-1}$ h$^{-1}$) (physiological absorption) and data on the arbuscular mycorrhizal (AM: 10–81%) fungi colonization (biotic absorption) were also used. Methods for measuring root morphology, root phosphatase activity, and mycorrhizal colonization are detailed in Lugli et al. (2020).

## 2.2 Structural Equation Models

Four hypothetical structural models were developed, called model A (Fig. 1), model B (Fig. 2), model C (Fig. 3), and model D (Fig. 4). The first three models (A, B, and C) were constituted by the latent variables: root morphology pool,

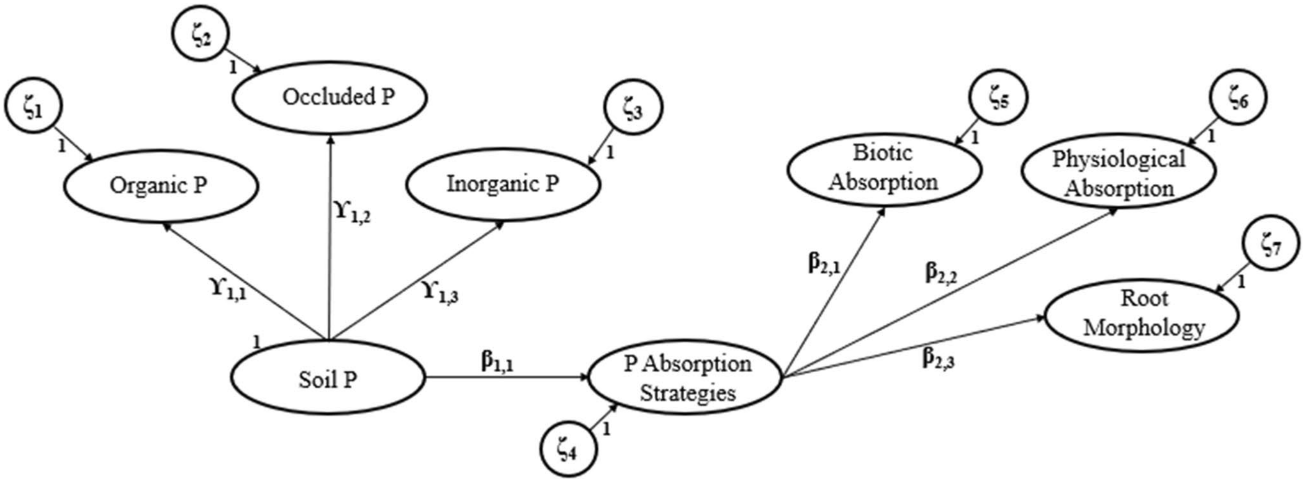

**Fig. 1** Model A: Theoretical structural model of the influence of soil P on plant absorption strategies. Latent variables are represented in circles or ellipses. The values correspond to the standardized estimated parameters ($p < 0.001$), with factorial loads $\Upsilon$ and $\beta$ between exogenous and endogenous; $\zeta$ are the error variations of the endogenous latent variables

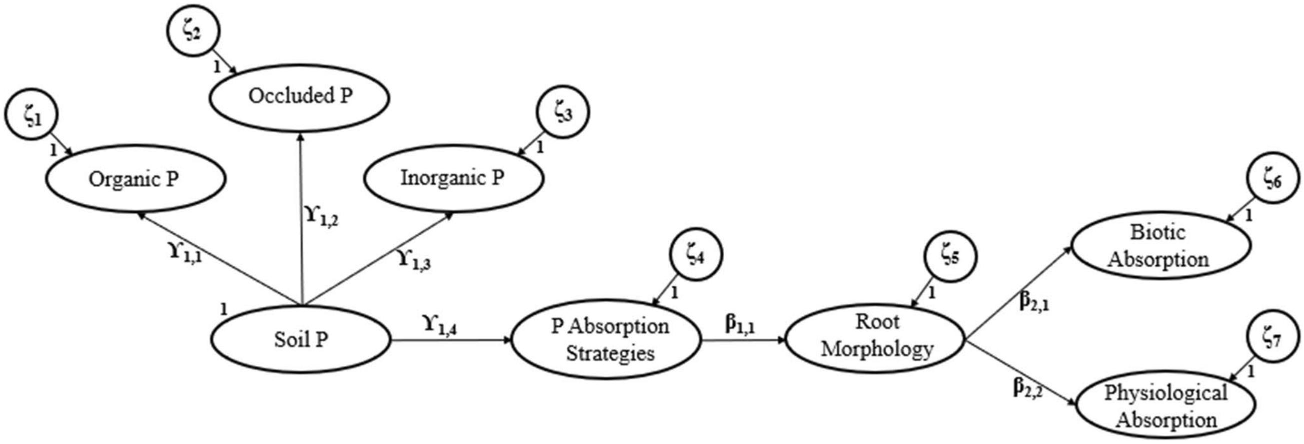

**Fig. 2** Model B: Theoretical structural model of the influence of soil P on plant absorption strategies, and this on root morphology, biotic, and physiological absorption. Latent variables are represented in circles or ellipses. The values correspond to the standardized estimated parameters ($p < 0.001$), with factorial loads $\Upsilon$ and $\beta$ between exogenous and endogenous; $\zeta$ are the error variations of the endogenous latent variables

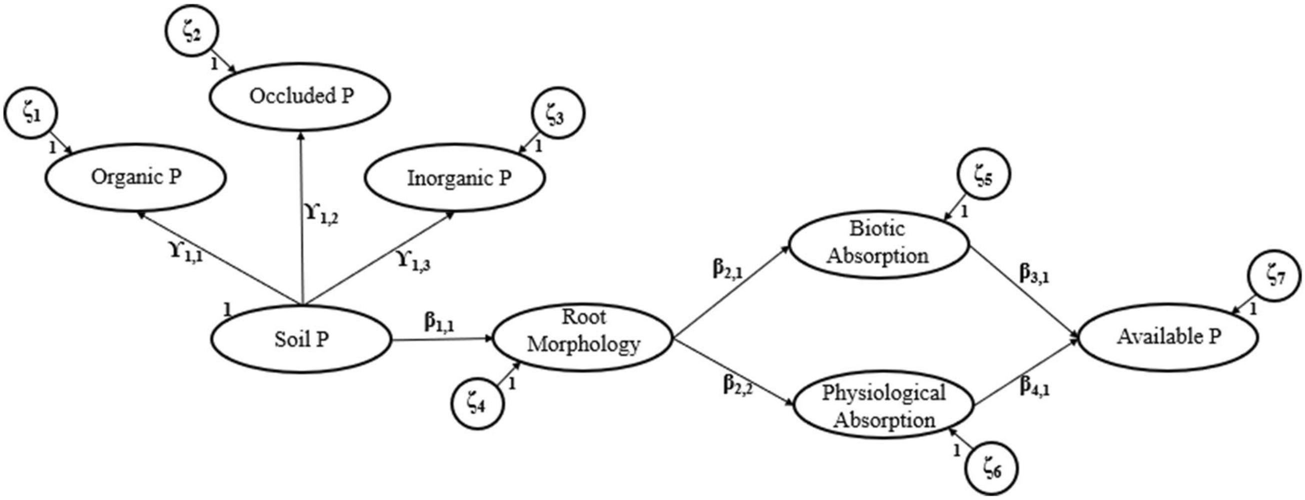

**Fig. 3** Model C: Theoretical structural model of the influence of soil P on root morphology, biotic and physiological absorption, and P available. Latent variables are represented in circles or ellipses. The values related to the standardized estimated parameters ($p < 0.001$), with factor loads $\Upsilon$ and $\beta$ between exogenous and endogenous; $\zeta$ are the error variations of the endogenous latent variables

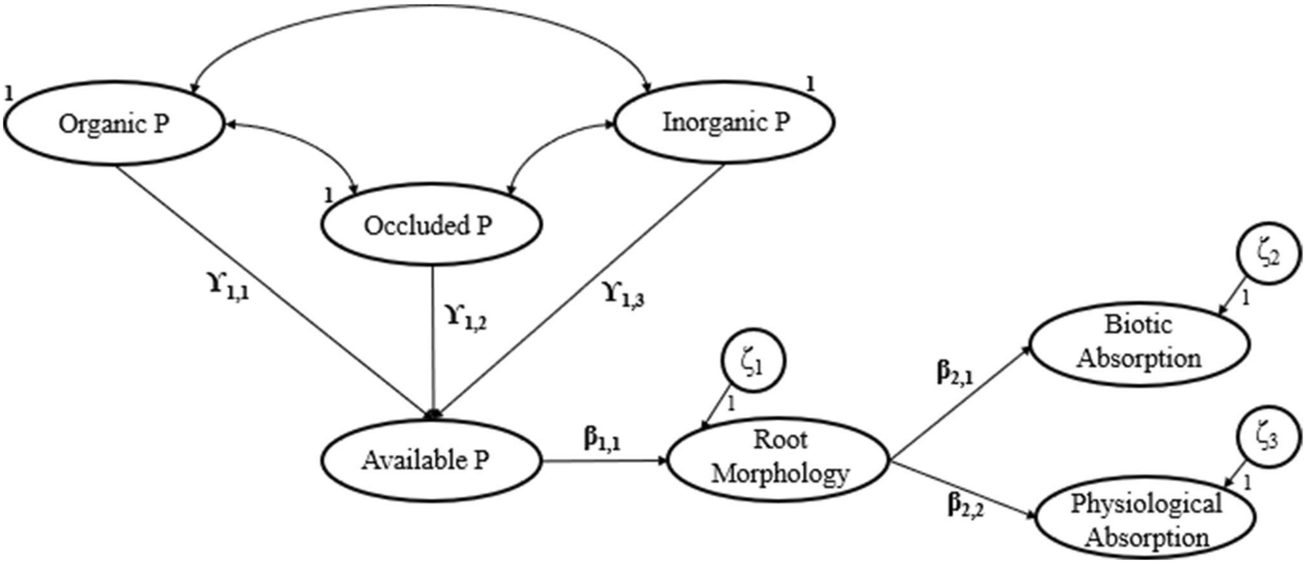

**Fig. 4** Model D: Alternative theoretical structural model of the influence of soil P on available P, and this on root morphology, biotic, and physiological absorption. Latent variables are represented in circles or ellipses. The values related to the standardized estimated parameters ($p < 0.001$), with factor loads $\Upsilon$ and $\beta$ between exogenous and endogenous; $\zeta$ are the error variations of the endogenous latent variables

physiological absorption pool, biotic absorption pool, and P pool, which conceptually represents all soil P forms, specifically affecting three pools of the P cycle: organic P ($P_o$), inorganic P ($P_i$), and occluded P. The $P_o$, $P_i$, and occluded P pools are latent exogenous variables and available P pool is latent endogenous variable in model D (Fig. 4). Additionally, submodels (Supplementary material) were developed to demonstrate the degree of influence between the P cycle variables (Submodel 1 — Figure S1) and between the plant P-absorption strategies (Submodel 2 — Figure S2) in parts, and thus present how the four tested hypothetical structural models were developed.

A convergent analysis of the constructs was performed to indicate how well a latent variable (constructs) was developed. This analysis manages to assess the reflection degree of the theoretical construct which should be measured by these variables (Hair et al. 2009). Convergence was calculated using indicators associated with the quality of a standardized structural model, being represented by the extracted variance (*EV*) and the construct reliability (*CR*). The *EV* calculation (1) will indicate the convergent validity and how much the constructs can explain the variance of the indicators, represented by:

$$EV = \frac{\sum_{i=1}^{n} \lambda_i^2}{\sum_{i=1}^{n} \lambda_i^2 + \sum_{i=1}^{n} \varepsilon_i} \tag{1}$$

Another indicator of convergent validity that is also used is the *CR*, and can be calculated using Eq. (2).

$$CR = \frac{\left(\sum_{i=1}^{n} \lambda_i\right)^2}{\left(\sum_{i=1}^{n} \lambda_i\right)^2 + \left(\sum_{i=1}^{n} \varepsilon_i\right)} \tag{2}$$

In both calculations, there is a representation of $\lambda$ = standardized factor loading, $i$ = item number, and $\varepsilon$ = random error of each indicator of the construct. Adequate convergence is achieved with *EV* values $\geq 0.5$; *CR* values $\geq 0.7$ are considered good, and values between 0.6 and 0.7 are acceptable (Hair et al. 2009).

The AMOS version 22 software program (IBM-SPSS Inc., Chicago, IL, USA) was used for the SEM analysis. The model parameters were estimated using the generalized least squares (GLS) method. Some goodness-of-fit indices were used to validate each estimated model, such as the chi-squared test ($X^2$), the degrees of freedom (*df*), and the probability level (*p*), which according to Sales et al. (2017) indicates a good fit when accepting the null hypothesis ($p > 0.05$). As an alternative to these indices, and given the high sensitivity of the $X^2$ test to the sample size, we also used for the adequacy of the models the $X^2/df$ ratio standardizing values < 3 (Iacobucci 2009), the goodness-of-fit index (GFI) with values $\geq 0.95$ (Hair et al. 2009), and the root-mean-square error of approximation (RMSEA) considering values $\leq 0.10$ (Byrne 2009). The data set was composed of $n = 32$ without the need for transformation, and the multivariate normality were obtained through the critical relation (*cr*) data, which had default values < 5 (Byrne 2009).

## 3 Results

The four hypothetical structural models (Figs. 1, 2, 3 and 4) showed satisfactory fit indices (Figs. 5, 6, 7, 8, 9 and 10; Table 1), confirming the relational hypotheses. In a general analysis of the *EV* and *CR* values (Table 1) of all models, it is verified that most of the constructs (latent) only presented

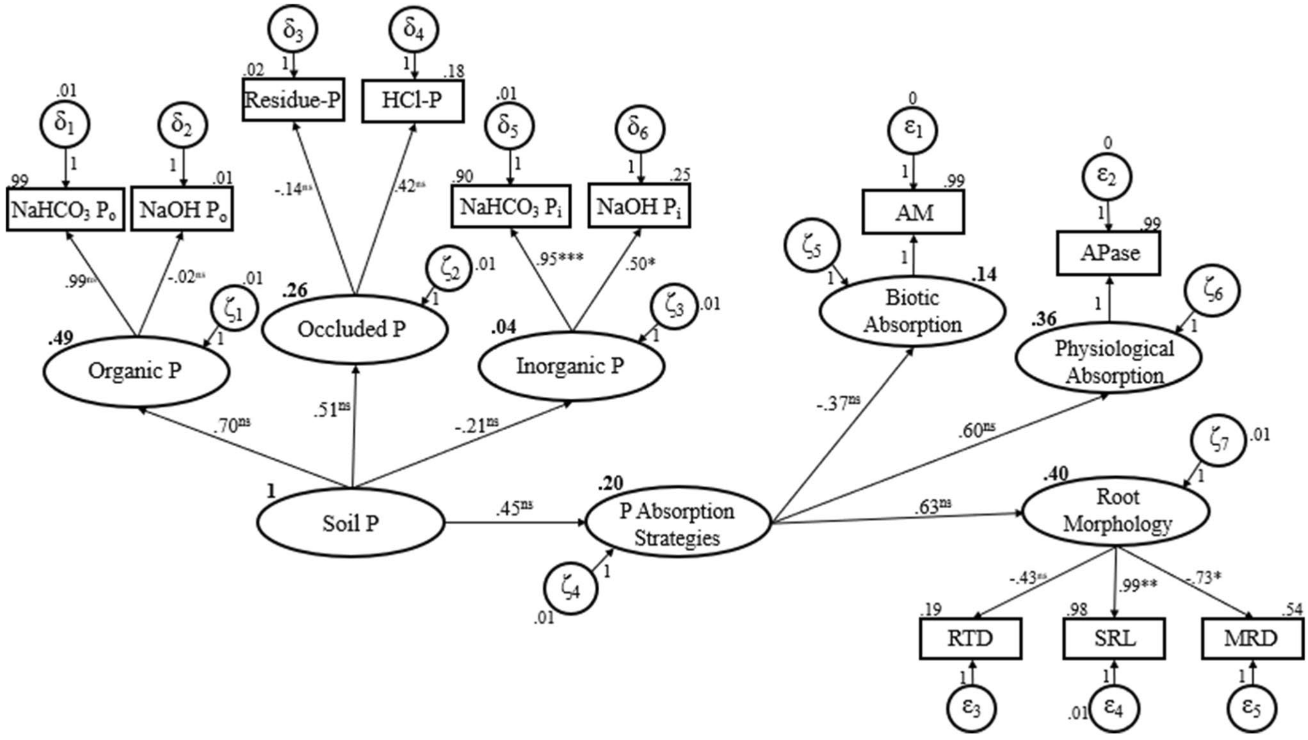

**Fig. 5** Model A: Structural model for the relationships between soil P (mg kg$^{-1}$), root morphology (SRL = specific root length (cm mg$^{-1}$); RTD = root tissue density (mg cm$^{-3}$); MRD = mean root diameter (mm)), biotic absorption (AM = arbuscular mycorrhizae (%)), and physiological absorption (APase = root acid phosphomonoesterase (nmol mg$^{-1}$ h$^{-1}$)). All measured variables (in boxes) are represented as indicators of effects associated with latent variables (in circles or ellipses). The values correspond to the standardized estimated parameters (***$p < 0.001$; **$p < 0.01$; *$p < 0.05$; ns — not significant) and the value of $R^2$ (numbers in bold). Values of error variables ($\delta_1$–$\delta_6$, $\varepsilon_1$–$\varepsilon_6$, $\zeta_1$–$\zeta_7$) are standardized; some errors were fixed at 0, 1, or 10%. Model $X.^2 = 37.52$; $df = 46$; $p = 0.809$; parameter = 18; $n = 32$

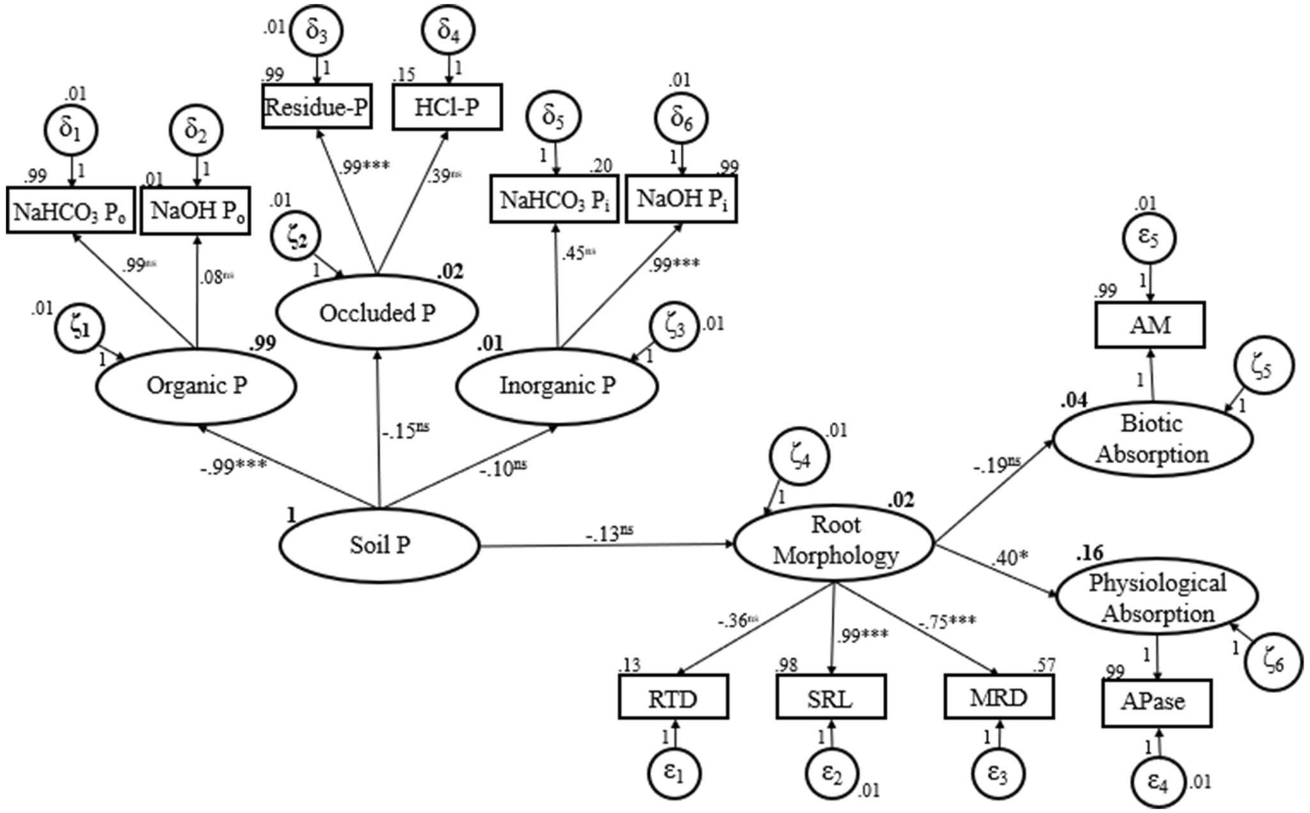

**Fig. 6** Model B: Structural model respecified for the relationships between soil P (mg $kg^{-1}$), root morphology (SRL = specific root length (cm $mg^{-1}$); RTD = root tissue density (mg $cm^{-3}$); MRD = mean root diameter (mm)), biotic absorption (AM = arbuscular mycorrhizae (%)), and physiological absorption (APase = root acid phosphomonoesterase (nmol $mg^{-1}$ $h^{-1}$)). All measured variables (in boxes) are represented as indicators of effects associated with latent variables (in circles or ellipses). The values correspond to the standardized estimated parameters (***$p < 0.001$; **$p < 0.01$; *$p < 0.05$; ns — not significant) and the value of $R^2$ (numbers in bold). Values of error variables ($\delta_1$–$\delta_6$, $\varepsilon_1$–$\varepsilon_6$, $\zeta_1$–$\zeta_7$) are standardized; some errors were fixed at 0, 1, or 10%. Model $X.^2 = 33$; $df = 43$; $p = 0.864$; parameter = 17; $n = 32$

fit in the *EV* values. These results define which constructs have internal consistency between the measured variables, and thus adequate representation (Hair et al. 2009).

The first hypothetical model (Fig. 1 — Model A) was identified and fitted (Fig. 5), confirming the interrelationships between the pools of P ($P_i$, $P_o$, and occluded P as latent indicator variables) and P absorption strategies (biotic absorption, physiological absorption, and root morphology as latent indicator variables). The results were consistent with the inference that the P absorption strategies pool (endogenous latent variable) was directly dependent on the P pool (exogenous latent variable). The relationship between the latent variable $P_i$ and the measurable variable $NaHCO_3$-$P_i$ was fixed at 1 to find a unique solution for the model, the $\delta_1$ and $\delta_5$ errors were respectively associated to the measurable variables $NaHCO_3$-$P_o$ and $NaHCO_3$-$P_i$, the $\varepsilon_4$ error was associated to the measurable variable SRL, and the $\zeta_1$, $\zeta_2$, $\zeta_3$, $\zeta_4$, and $\zeta_7$ errors were respectively associated to the latent variables $P_o$, occluded P, and $P_i$, P absorption strategies and root morphology, and were set at 1%; the $\varepsilon_1$ and $\varepsilon_2$ errors were respectively associated to the measurable variables AM and *APase* and fixed at 0%. The root morphology and physiological absorption pools were directly and positively dependent on the P absorption strategies pool, while the biotic absorption pool was directly and negatively dependent on the P absorption strategies pool. All three pools (root morphology, biotic absorption, and physiological absorption) were indirectly and positively dependent (via P absorption strategies) on the P pool, causing an overall effect $\beta = -0.54$ for the latent variable biotic absorption, $\beta = 0.87$ for the latent variable physiological absorption, and $\beta = 0.91$ for the latent variable root morphology. The model explained 14%, 36%, and 40% of the respective variances ($R^2$) of the biotic absorption, physiological absorption, and root morphology pools (Fig. 5).

There was no identification of the second hypothetical model (Fig. 2 — Model B). For this reason, a re-specification was performed to obtain a satisfactory fit (Fig. 6; Table 1) by eliminating the P absorption strategies pool. Thus, the respecified model showed direct interrelationships between

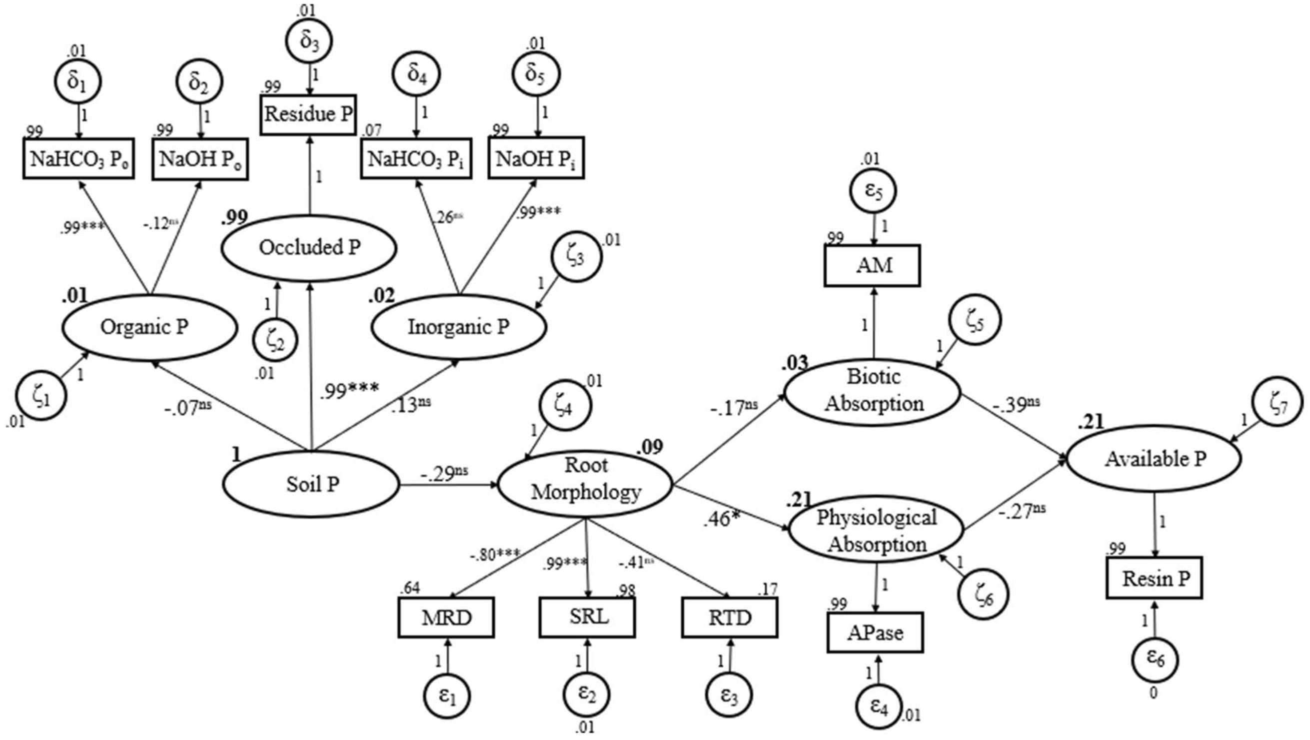

**Fig. 7** Model C: Structural model for the relationships between soil P (mg $kg^{-1}$), root morphology (SRL = specific root length (cm $mg^{-1}$); RTD = root tissue density (mg $cm^{-3}$); MRD = mean root diameter (mm)), biotic absorption (AM = arbuscular mycorrhizae (%)), and physiological absorption (APase = root acid phosphomonoesterase (nmol $mg^{-1}$ $h^{-1}$)). All measured variables (in boxes) are represented as indicators of effects associated with latent variables (in circles or ellipses). The values correspond to the standardized estimated parameters (***$p < 0.001$; **$p < 0.01$; *$p < 0.05$; ns — not significant) and the value of $R^2$ (numbers in bold). Values of error variables ($\delta_1$–$\delta_6$, $\varepsilon_1$–$\varepsilon_6$, $\zeta_1$–$\zeta_7$) are standardized; some errors were fixed at 0, 1, or 10%. Model $X.^2 = 38.47$; $df = 44$; $p = 0.707$; parameter = 19; $n = 32$

pools of P and root morphology. The results presented were consistent with the inference that the biotic absorption and physiological absorption pools were directly dependent on the root morphology pool, and indirectly dependent on the soil P pool. Indirect and negative soil P pool (via root morphology) caused an overall effect of $\beta = -0.16$ for the latent biotic absorption variable, and $\beta = 0.35$ for the latent physiological absorption variable. The model explained 4% and 16% of the respective variances ($R^2$) of the biotic absorption and physiological absorption pools (Fig. 6). In order to find a unique solution for the model, the relationship between the latent variable $P_o$ and the measurable variable $NaHCO_3$-$P_o$, and the latent variable occluded P and the measurable variable HCl-P were fixed at 1; the $\delta_1$ and $\delta_3$ and $\delta_6$ errors were respectively associated to the measurable variables $NaHCO_3$-$P_o$, Residual P, and NaOH-$P_i$; the $\varepsilon_2$, $\varepsilon_4$, and $\varepsilon_5$ errors were respectively associated to the measurable variables SRL, *APase*, and AM; and the $\zeta_1$, $\zeta_2$, $\zeta_3$, and $\zeta_4$ errors were respectively associated to the latent variables $P_o$, occluded P, $P_i$, and root morphology, and were fixed at 1%.

The third hypothetical model (Fig. 3 — Model C) was identified and satisfactorily fit (Table 1; Fig. 7). The model demonstrated the inference that the available P pool (endogenous latent variable) was directly dependent on the biotic and physiological absorption pools, indirectly dependent on the root morphology pool (both endogenous latent variables), and therefore indirectly dependent on the soil pool P (exogenous latent variable), causing an overall effect $\beta = -0.70$. The model explained only 21% of the variance ($R^2$) of the available P pool (Fig. 7). A single solution for the model was found by fixing the $\delta_1$, $\delta_3$, and $\delta_5$ errors at 1% and respectively associated to the measurable variables $NaHCO_3$-$P_o$, Residual P, and NaOH-$P_i$; the $\varepsilon_2$, $\varepsilon_4$, and $\varepsilon_5$ errors were respectively associated to the measurable variables SRL, *Apase*, and AM; and the $\zeta_1$, $\zeta_2$, $\zeta_3$, and $\zeta_4$ errors were respectively associated to the latent variables $P_o$, occluded P, $P_i$, and root morphology; and the $\varepsilon_6$ error was respectively associated to the measurable variable Resin-P and all were fixed at 0%.

A re-specification was performed to improve the fit of model C by adding a direct relationship between the available $P_o$ and P pools (Fig. 8 — Model C1). The model showed that the available P pool was directly and positively dependent on the $P_o$ pool. The relationships between the available P pool and the other pools in the model were similar to model C (Fig. 7). The soil P pool as an exogenous latent variable

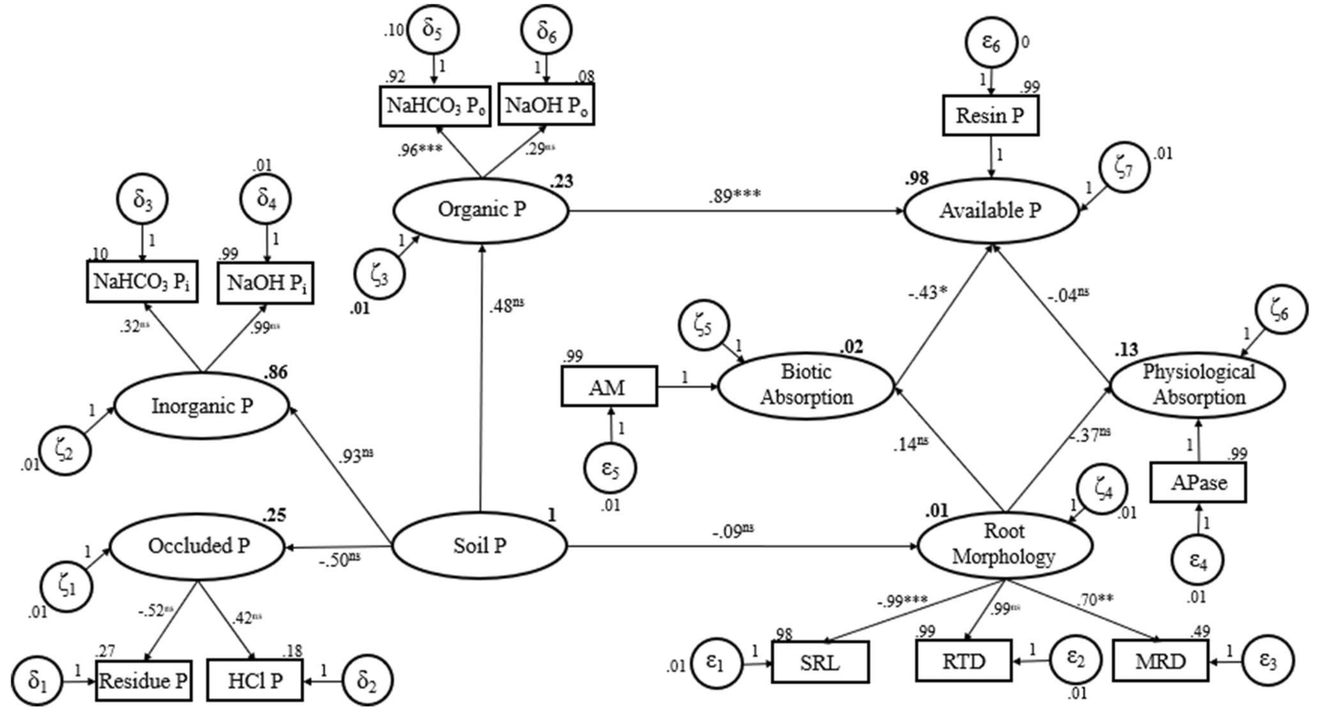

**Fig. 8** Model C1: Structural model respecified for the relationships between soil P (mg kg$^{-1}$), root morphology (SRL = specific root length (cm mg$^{-1}$); RTD = root tissue density (mg cm$^{-3}$); MRD = mean root diameter (mm)), biotic absorption (AM = arbuscular mycorrhizae (%)), and physiological absorption (APase = root acid phosphomonoesterase (nmol mg$^{-1}$ h$^{-1}$)). All measured variables (in boxes) are represented as indicators of effects associated with latent variables (in circles or ellipses). The values correspond to the standardized estimated parameters (***$p < 0.001$; **$p < 0.01$; *$p < 0.05$; ns — not significant) and the value of $R^2$ (numbers in bold). Values of error variables ($\delta_1$–$\delta_6$, $\varepsilon_1$–$\varepsilon_6$, $\zeta_1$–$\zeta_7$) are standardized; some errors were fixed at 0, 1, or 10%. Model $X.^2 = 49.22$; $df = 54$; $p = 0.659$; parameter = 21; $n = 32$

caused an overall effect $\beta = 0.80$ on the available P pool. The model explained 98% of the variance ($R^2$) of the available P pool (Fig. 8). In order to find a unique solution for the model, the relationship between the latent variable occluded P and the measurable variable HCl-P was fixed at 1; the $\delta_5$ error associated with the measurable variable NaHCO$_3$-P$_o$ was set at 10%; the $\delta_4$ error was associated with the measurable variable NaOH-P$_i$; the $\varepsilon_1$, $\varepsilon_2$, $\varepsilon_4$, and $\varepsilon_5$ errors were respectively associated to the measurable variables SRL, RTD, *Apase*, and AM, and the $\zeta_1$, $\zeta_2$, $\zeta_3$, $\zeta_4$, and $\zeta_7$ errors were respectively associated to the latent variables occluded P, P$_i$, P$_o$, root morphology, and available P, and fixed at 1%; lastly, the $\varepsilon_6$ error associated to the measurable variable Resin-P was fixed at 0%.

A second re-specification of model C (Fig. 7) was performed with the addition of a direct relationship between the P$_o$ pools and physiological absorption, and the measurable variable HCl-P associated with the latent variable occluded P was eliminated; the inversion of the relationships of the available P pool with the biotic absorption and physiological absorption pools then became the model's response variables (Fig. 9 — Model C2). With these modifications, the model presented the inference that the biotic absorption pool (endogenous latent variable) was directly dependent on the root morphology and available P (endogenous latent variables) pools, and indirectly dependent on the P$_o$ (endogenous latent variable) and P pools (exogenous latent variable). While the physiological absorption pool (endogenous latent variable) was directly dependent on the root morphology, available P and P$_o$ pools, and indirectly dependent on the soil P pool. These structural relationships caused an overall effect $\beta = -0.38$ and $\beta = -0.28$, respectively, on the biotic absorption and physiological absorption pools. The model explained 27% of the variance ($R^2$) of the biotic absorption pool and 48% of the physiological absorption pool. To find a unique solution for the model, the relationship between the latent variable P$_i$ and its measurable variable NaHCO$_3$-P$_i$ was fixed at 1; the $\delta_1$ and $\delta_3$ errors were respectively associated with the measurable variables Residual P and NaOH-P$_i$; the $\varepsilon_1$, $\varepsilon_2$, $\varepsilon_4$, and $\varepsilon_5$ errors were respectively associated to the measurable variables SRL, RTD, *APase*, and AM; and the $\zeta_1$, $\zeta_2$, $\zeta_3$, and $\zeta_4$ errors were respectively associated to the latent variables occluded P, P$_i$, P$_o$, and root morphology, and were fixed at 1%; the $\varepsilon_6$ error associated to the measurable variable Resin-P was fixed at 0%.

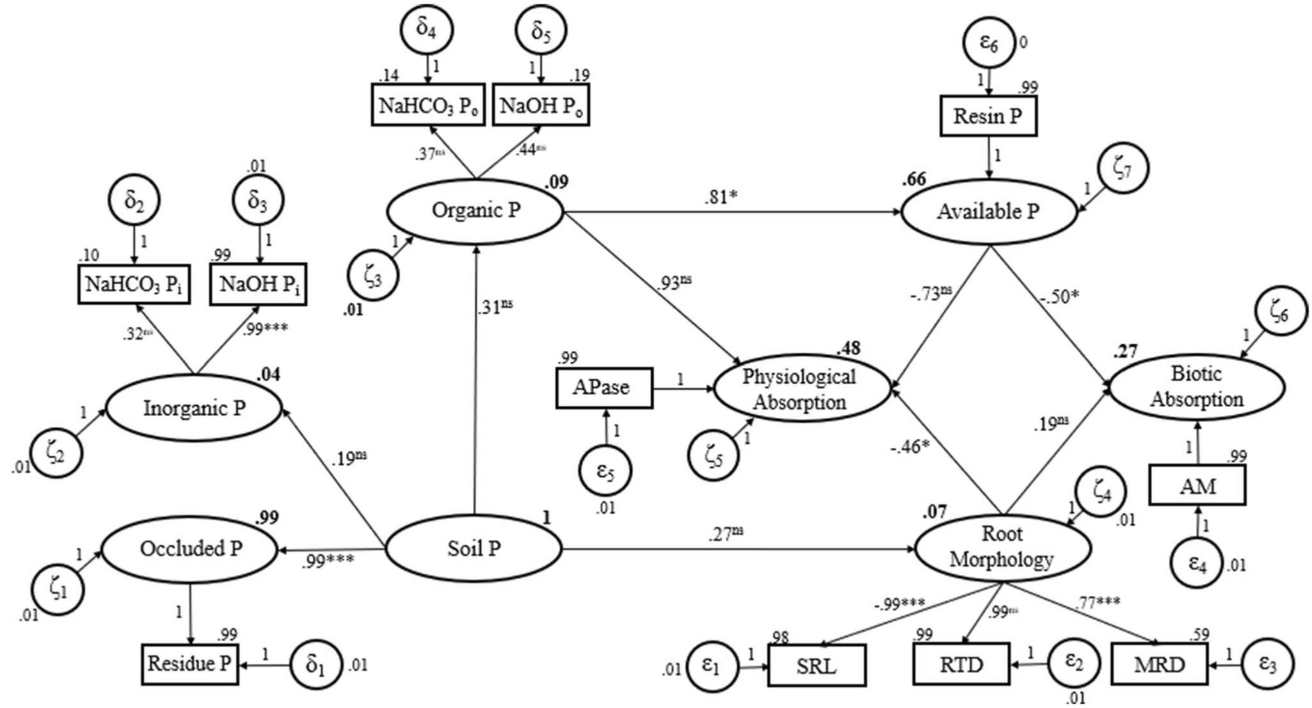

**Fig. 9** Model C2: Structural model respecified for the relationships between soil P (mg $kg^{-1}$), root morphology (SRL = specific root length (cm $mg^{-1}$); RTD = root tissue density (mg $cm^{-3}$); MRD = mean root diameter (mm)), biotic absorption (AM = arbuscular mycorrhizae (%)), and physiological absorption (APase = root acid phosphomonoesterase (nmol $mg^{-1}$ $h^{-1}$). All measured variables (in boxes) are represented as indicators of effects associated with latent variables (in circles or ellipses). The values correspond to the standardized estimated parameters (***$p < 0.001$; **$p < 0.01$; *$p < 0.05$; ns — not significant) and the value of $R^2$ (numbers in bold). Values of error variables ($\delta_1$–$\delta_6$, $\varepsilon_1$–$\varepsilon_6$, $\zeta_1$–$\zeta_7$) are standardized; some errors were fixed at 0, 1, or 10%. Model $X.^2 = 38.98$; $df = 43$; $p = 0.646$; parameter = 21; $n = 32$

The fourth hypothetical model (Fig. 4 — Model D) was identified and satisfactorily fit (Table 1; Fig. 10). The model demonstrated the inference that the biotic and physiological absorption pools were directly dependent on the root morphology pool (endogenous latent variable), indirectly dependent on the available P pool (endogenous latent variable), and indirectly dependent on exogenous latent variables, the $P_o$, $P_i$, and occluded P pools, causing an overall effect $\beta = -0.70$. The model explained only 3% and 16%, respectively, of the variances ($R^2$) of the biotic absorption and physiological absorption pools, but there was a high explanation ($R^2 = 94\%$) of the available P pool (Fig. 10). A single solution for the model was found by the $\delta_1$, $\delta_3$, and $\delta_4$ errors being respectively associated with the measurable variables $NaHCO_3$-$P_o$, residual P, and NaOH-$P_i$; the $\varepsilon_3$, $\varepsilon_5$, and $\varepsilon_6$ errors, respectively, associated to the measurable variables SRL, *APase*, and AM; and the $\zeta_2$ error associated to the latent variable root morphology and fixed at 1%. The $\varepsilon_1$ error associated with the measurable variable Resin-P was fixed at 0%.

Two submodels were developed with satisfactory fit indices (Table S1; Figures S1 and S2). Submodel 1 (Figure S1) shows only the P cycle, in which the available P pool was directly and positively dependent on the $P_o$, $P_i$, and occluded P pools. The $\delta_2$, $\delta_3$, and $\delta_5$ errors associated respectively with the measurable variables NaOH-$P_o$, Residual P, and NaOH-$P_i$ were set at 1%, and the $\varepsilon_1$ error associated with the measurable variable resin-P was set at 0% in order to find a single solution for the model. The submodel explained 44% of the variance in the available P pool, and an overall effect $\beta = 0.92$. Submodel 2 (Figure S2) confirms the conceptual latent variable P absorption strategies and the interdependence of its indicator latent variables (physiological absorption, root morphology, and biotic absorption pools). To find a single solution for the submodel, the $\varepsilon_2$, $\varepsilon_4$, and $\varepsilon_5$ errors, respectively, associated with the measurable variables SRL, AM, and *APase* were set at 1%, and the $\zeta_3$ error was associated with the latent variable root morphology. The submodel explained 8%, 65%, and 36%, respectively, of the variances of the biotic absorption, physiological absorption, and root morphology pools, with an overall effect $\beta = 1.13$.

## 4 Discussion

### 4.1 Fitted Structural Models

The general fit of all structural models (Figs. 5–10; Table 1) confirms the theoretical concept of interdependence between

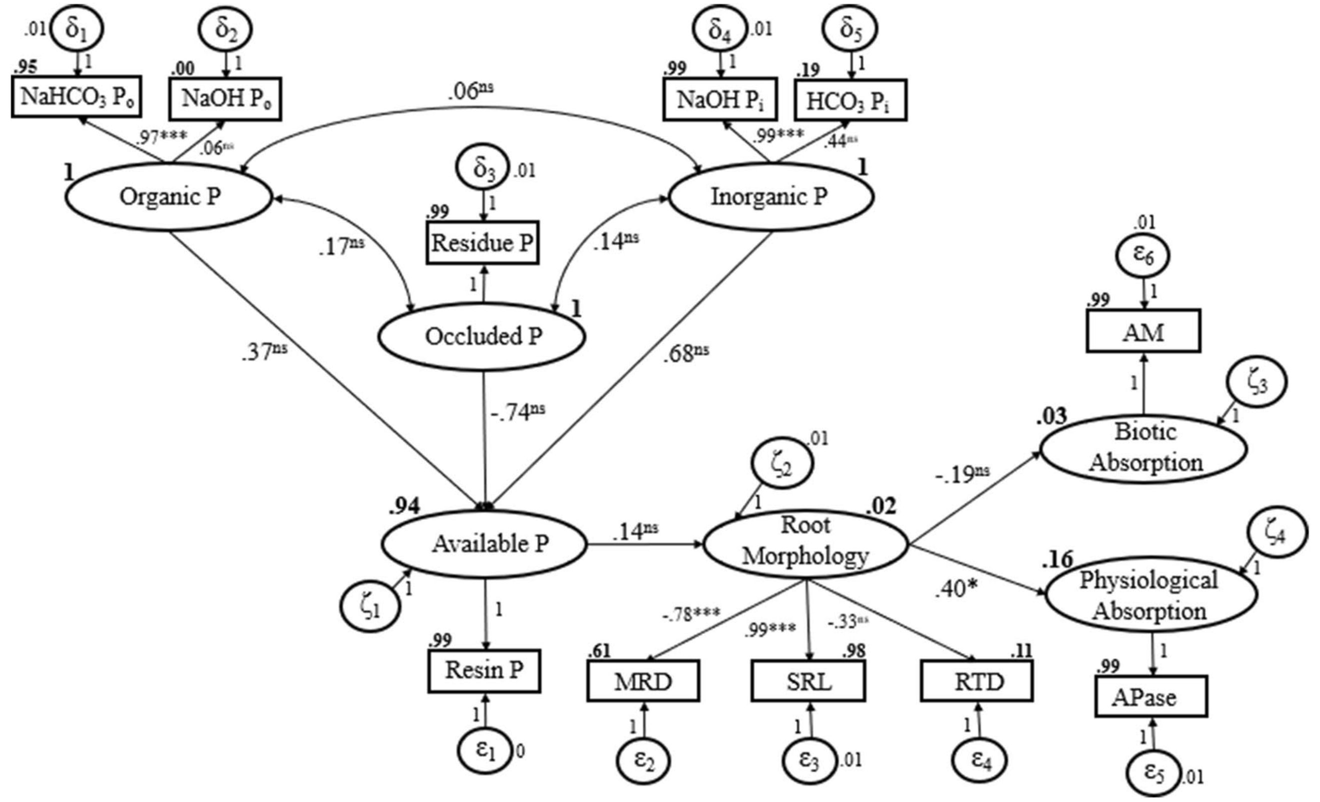

**Fig. 10** Model D: Structural model for the relationships between soil P cycle and plant P-absorption strategies. Acronyms: Root morphology (SRL = specific root length; RTD = root tissue density; MRD = mean root diameter), biotic absorption (AM = arbuscular mycorrhizae), and physiological absorption (APase = root acid phosphomonoesterase). All measured variables (in rectangles) are represented as indicators of effects associated with latent variables (in circles or ellipses). The values correspond to the standardized estimated parameters (***$p<0.001$; **$p<0.01$; *$p<0.05$; ns —not significant) and the value of $R^2$ (numbers in bold). The values of the error variables ($\delta_1$–$\delta_5$, $\varepsilon_1$–$\varepsilon_6$, $\zeta_1$–$\zeta_4$) are standardized; some errors were fixed at 0, 1, or 10%. Model $X.^2=47.62$; $df=43$; $p=0.290$; parameter = 20; $n=32$

**Table 1** Fit indices, multivariate normality, and construct reliability of the structural models (A–D) of plant strategies for P absorption in Amazon Forest soils

| Model | Fit indices* | | | | | | Multivariate normality* | |
|---|---|---|---|---|---|---|---|---|
| | *$X^2$* | *df* | *p* | *$X^2$/df* | *GFI* | *RMSEA* | *cr* | |
| A (Fig. 5) | 37.52 | 46 | 0.809 | 0.81 | 0.78 | < 0.001 | 0.58 | |
| B (Fig. 6) | 33.00 | 43 | 0.864 | 0.76 | 0.80 | < 0.001 | 0.58 | |
| C (Fig. 7) | 38,47 | 44 | 0.707 | 0.87 | 0.77 | < 0.001 | 0.90 | |
| C1 (Fig. 8) | 49.22 | 54 | 0.659 | 0.91 | 0.73 | < 0.001 | 0.96 | |
| C2 (Fig. 9) | 38.98 | 43 | 0.646 | 0.90 | 0.77 | < 0.001 | 0.90 | |
| D (Fig. 10) | 47.62 | 43 | 0.290 | 1.10 | 0.72 | 0.059 | 0.60 | |
| | Construct reliability* (%) | | | | | | | |
| | Organic-P | | Inorganic-P | | Occluded-P | | Root morphology | |
| | *VE* | *CR* | *VE* | *CR* | *VE* | *CR* | *VE* | *CR* |
| A (Fig. 5) | 50 | 54 | 60 | 72 | 58 | 69 | 56 | 01 |
| B (Fig. 6) | 50 | 49 | 58 | 71 | 10 | 04 | 57 | 02 |
| C (Fig. 7) | 50 | 44 | 53 | 63 | - | - | 60 | 04 |
| C1 (Fig. 8) | 50 | 61 | 55 | 66 | 45 | 37 | 82 | 49 |
| C2 (Fig. 9) | 17 | 28 | 55 | 66 | - | - | 86 | 59 |
| D (Fig. 10) | 47 | 50 | 60 | 72 | - | - | 57 | 01 |

*Pattern: $X^2$ = smaller possible; df ≥ 0; $p>0.05$; $X^2$/df ≤ 3; GFI ≥ 0.95; RMSEA ≤ 0.10; *cr* < 5; VE ≥ 0.5; CR ≥ 0.7

P pools ($P_i$, $P_o$, and occluded P) and pools with different P absorption strategies used by Amazon rainforest in P-impoverished soils. Simplifying the demonstrations of the various variables which act in regulating the P cycle in the soil was made possible by using latent variables in the models, in turn facilitating estimating and reducing measurement errors. Low values found for construct reliability (*CR*) and extracted variance (*EV*) for some latent variables can be attributed to other variables external to the model (Table 1). Thus, when it is not possible to reach the *CR* and *EV* index, it is assumed that a single underlying cause is not consistent between the correlations or covariances of the indicator variables (Oliveira et al. 2018). A single model does not have the capacity to estimate the complex interdependence of transformations that can occur with soil P and all the strategies that plants can develop to absorb the element, but the theoretical concept (multivariate hypothesis) can be confirmed by choosing the model that best represents the theory through approximate fits or some changes in the component variables (Sales et al. 2017).

### 4.2 Holistic View of the Relationships Between the P Cycle in Soil and Plant Uptake Strategies

The use of SEM enabled a holistic view of all the relationships involving the soil P cycle together with the strategies that plants have to improve efficiency in nutrient absorption. All fitted structural models showed the simultaneous integration of the variables involved in the P absorption strategies in the soil represented by root morphology, mycorrhizal symbiosis, and enzymatic exudation. These models corroborate the suggestion by Wen et al. (2019) that the best way to understand the strategies for obtaining P in the soil is precisely through this holistic view of the functional characteristics of the root system. Furthermore, our models brought to light theoretical propositions, such as the possibility of a direct and simultaneous relationship between investments in root morphology and the P absorption strategies. In turn, Lugli et al. (2020) did not integrate the P cycle with the P acquisition strategies, leading them to the conclusion that root morphology has a strong relationship with acid phosphatase in the analyzed soils, but does not interfere with mycorrhizal symbiosis. Furthermore, both the hydrolysis of $P_o$ and the acquisition of $P_i$ by mycorrhizal fungi were attributed as complementary mechanisms. However, our models demonstrated that root morphology has a significant and simultaneous influence on mycorrhizal fungi and acid phosphomonoesterase activity and that $P_o$ is the main source of P for maintaining the forest ecosystem, since the organic fraction represented 48.4% of the total P extracted by Hedley fractionation.

Model C1 (Fig. 8) showed that the direct relationship between the available $P_o$ and P pools significantly increased the variance ($R^2$) of the available P pool (model response variable), confirming that this relationship arising from the $P_o$ turnover is critical to regulating the availability of P in the soil. In model C2 (Fig. 9), the direct and negative relationship of the available P pool to the biotic absorption and physiological absorption pools (model response variables) showed that the low availability of P in the soil would stimulate both an increase in *APase* activity, as well as for the mycorrhizal association; therefore, the activities of these enzymes and fungi are inherent in low-P soils. In addition, the direct and positive relationship of the $P_o$ pool to the physiological absorption pool shows that not only the P-availability, but also the size of the organic substrate would affect *APase* activity. Moreover, the size of the $P_o$ pool would indirectly affect the biotic absorption pool (Figs. 8 and 9 — Models C1 and C2). Arbuscular mycorrhizal fungi also synthesize phosphatase enzymes and thus can use $P_o$ as a source of P (Liu et al. 2018; Richardson et al. 2009; Turner 2008; Yazdani et al. 2009). Therefore, mycorrhizal fungi can play a dual role in P uptake strategies, such as accelerating $P_i$ uptake, expanding plant exploitation limits, and solubilizing $P_o$ (Smith et al. 2011; Zhang et al. 2018), characterizing a complementary function in conjunction with the physiological absorption strategy (*APase*). Alternative model D (Fig. 10) showed the plausibility of the direct structural relationship of the available P pool over the root morphology pool, and therefore to the other P absorption strategies in the Amazon forest site, although the model did not present a better fit compared to other models.

Except for model A (Fig. 5), both biotic and physiological absorption pools are simultaneously affected by the root morphology pool in all other models (Figs. 6, 7, 8 and 9); therefore, they are interconnected through an inverse relationship between the measurable variables *APase* and AM. The models showed that all P absorption strategies simultaneously manifest themselves at the ecosystem level, but the predominance of a given strategy will depend on the metabolic cost/benefit balance as a function of P transformations in the soil of the forest site. Thus, if the plant preferentially invests (positive relationship) in physiological absorption, the intensity of biotic absorption would consequently tend to decrease (negative relationship), depending on the costs and benefits of each process (Han et al. 2021; Nasto et al. 2017; Wen et al. 2022). The costs (i.e. energy) of using each of the strategies, despite contributing to increased P uptake in the soil, can restrict the ability of plants to manifest all of them at the same time (Han et al. 2021; Lynch and Ho 2005; Raven et al. 2018; Ryan et al. 2012). However, tree species at the tropical ecosystem-level from a particular forest site may show greater variability in enzymatic activity (Guilbeault-Mayers et al., 2020) or mycorrhizal association

(Nasto et al., 2017) compared to other sites in the same ecosystem, which does not reduce interspecific competition, but can benefit the acquisition of P forms ($P_o$ or $P_i$) according to nutrient availability and the contribution of different absorption strategies (Nasto et al. 2017; Turner 2008; Wen et al. 2022). Root phosphatase exudation is relatively more important in soils with low $P_i$ availability and high substrate availability, while AM fungi associations are relatively more important in soils with intermediate soil $P_i$ availability in Amazonia forest (Reichert et al. 2022). On the other hand, root productivity and traits related to nutrient acquisition strategies are not only affected by the $P_i$ availability, but can also be affected by the soil nutrient status. Lugli et al. (2021) reported that additions of P and cations (K, Ca, Mg) increased root productivity, root diameter, and mycorrhizal colonization, but decreased root phosphatase activity; in turn, no response was detected with N addition in Central Amazonia after 1 year of fertilization.

Thus, further research is needed to refine the fitted structural models, considering the influence of a soil P gradient, and add new variables, such as root organic acid exudation, which is important for accessing the occluded and organic P pools (Sales et al. 2017; Rinaldi et al. 2021); the fine root turnover rate, important in high-$P_i$ soils (Freschet et al. 2021); and plant P use, important for plants in low-P soils (Reichert et al. 2022). These environments have many unique characteristics and understanding how the various variables related to P-availability in the soil act is extremely important so that new hypotheses are proposed and help in understanding the efficiency of phosphorus absorption and the sustainability of the Amazon forest ecosystem.

## 5 Conclusion

Structural equation modeling with latent variables was able to simplify the relationship between the P cycle and plant strategies for P acquisition, and thus provide a holistic view of these mechanisms in P-impoverished environments. The fitted models made it possible to retrieve information which until then had not been considered, such as the P absorption strategy pool, which is an entirely conceptual latent variable, and the confirmation of a direct relationship between investments in root morphology and P-absorption strategies, demonstrating that root morphology (SRL, MRD, and RTD) has a strong influence on arbuscular mycorrhizal fungi (AM) and acid phosphomonoesterase (*APase*), and that $P_o$ was the main source of P for the maintenance of the Amazon forest ecosystem.

**Supplementary Information** The online version contains supplementary material available at https://doi.org/10.1007/s42729-022-00890-0.

**Acknowledgements** Any use of trade, firm, or product names is for descriptive purposes only. The authors thank the anonymous reviewers for their comments and suggestions on the manuscript.

**Funding** We received a research fellowship from the Conselho Nacional de Desenvolvimento Científico e Tecnológico — CNPq (Grant 302784/2017–9) awarded to Antonio Carlos Gama-Rodrigues and a postdoctoral scholarship from the Coordenação de Aperfeiçoamento de Pessoal de Nível Superior — CAPES (Grant 88882.14549/2019–01).

**Availability of Data and Material** Applicable.

**Code Availability** Not applicable.

## Declarations

**Conflict of Interest** The authors declare no competing interests.

## References

Bünemann E, Condron L (2007) Phosphorus and sulphur cycling in terrestrial ecosystems. In: Marschner P and Rengel Z (Eds). Nutrient cycling in terrestrial ecosystems. Springer, New York, pp 65–94. https://doi.org/10.1007/978-3-540-68027-7_3

Byrne BM (2009) Structural equation modeling with AMOS: basic concepts, applications and programming, 2nd edn. Routledge, New York

Clark RB, Zeto SK (2000) Mineral acquisition by arbuscular mycorrhizal plants. J Plant Nutr 23:867–902. https://doi.org/10.1080/01904160009382068

Condron LM, Turner BL, Cade-Menun BJ (2005) Chemistry and dynamics of soil organic phosphorus. In: Sims JT, Sharpley AN (Eds). Phosphorus: agriculture and the environment. American Society of Agronomy, Crop Science Society of America, Soil Science Society of America, Inc., Madison, pp 87–121. https://doi.org/10.2134/agronmonogr46.c4

Costa MG, Gama-Rodrigues AC, Gonçalves JLM, Gama-Rodrigues EF, Sales MVS, Aleixo S (2016) Labile and non-labile fractions of phosphorus and its transformations in soil under Eucalyptus plantations. Brazil Forests 7:15. https://doi.org/10.3390/f7010015

de Mesquita Filho MV, Torrent J (1993) Phosphate sorption as related to mineralogy of a hydrosequence of soils from the Cerrado region (Brazil). Geoderma 58:107–123. https://doi.org/10.1016/0016-7061(93)90088-3

Driessen P, Deckers J, Spaargaren O, Nachtergaele F (2001) Lecture notes on the major soils of the world. FAO, Rome, pp 35–37

Freschet GT, Roumet C, Comas LH, Weemstra M, Bengough AG et al (2021) Root traits as drivers of plant and ecosystem functioning: current understanding, pitfalls and future research needs. New Phytol 232:1123–1158

Gama-Rodrigues AC, Sales MVS, Silva PSD, Comerford NB, Cropper WP, Gama-Rodrigues EF (2014) An exploratory analysis of phosphorus transformations in tropical soils using structural equation modeling. Biogeochemistry 118:453–469. https://doi.org/10.1007/s10533-013-9946-x

George TS, Giles CD, Menezes-Blackburn D, Condron LM, Gama-Rodrigues AC et al (2018) Organic phosphorus in the terrestrial environment: a perspective on the state of art and future priorities. Plant Soil 427:191–208. https://doi.org/10.1007/s11104-017-3391-x

Grace JB, Bollen KA (2006) The interface between theory and data in structural equation models: U. S. Geological Survey Open-File Report 2006–1363, 33 p

Grace JB, Anderson TM, Olff H, Scheiner SM (2010) On the specification of structural equation models for ecological systems. Ecol Monogr 80:67–87. https://doi.org/10.1890/09-0464.1

Grace JB, Adler PB, Harpole WS, Borer ET, Seabloom EW (2014) Causal networks clarify productivity–richness interrelations, bivariate plots do not. Func Ecol 28:787–798. https://doi.org/10.1111/1365-2435.12269

Guilbeault-Mayers X, Turner BL, Lalibert E (2020) Greater root phosphatase activity of tropical trees at low phosphorus despite strong variation among species. Ecology 101:e03090. https://doi.org/10.1002/ecy.3090

Hair JF, Black WC, Babin BJ, Anderson E, Tathan RL (2009) Multivariate data analysis. Translation: Adonai Schlup Sant'Anna, 6. ed., Bookman, Porto Alegre

Haling RE, Brown LK, Stefanski A, Kidd DR, Ryan MH, Sandral GA, George TS, Lambers H, Simpson RJ (2018) Differences in nutrient foraging among *Trifolium subterraneum* cultivars deliver improved P-acquisition efficiency. Plant Soil 424:539–554. https://doi.org/10.1007/s11104-017-3511-7

Han M, Chen Y, Li R, Yu M, Fu L, Li S, Su J, Zhu B (2021) Root phosphatase activity aligns with the collaboration gradient of the root economics space. New Phytol. https://doi.org/10.1111/nph.17906

Hedley MJ, Stewart WB, Chauhan BS (1982) Changes in inorganic and organic soil phosphorus fractions induced by cultivation practices and by laboratory incubations. Soil Sci Soc Am J 46:970–976. https://doi.org/10.2136/sssaj1982.03615995004600050017x

Hinsinger P, Plassard C, Tang CX, Jaillard B (2003) Origins of root-mediated pH changes in the rhizosphere and their responses to environmental constraints: a review. Plant Soil 248:43–59. https://doi.org/10.1023/A:1022371130939

Iacobucci D (2009) Everything you always wanted to know about SEM (structural equations modeling) but were afraid to ask. J Consum Psychol 19:673–680. https://doi.org/10.1016/j.jcps.2009.09.002

Liu X, Burslem DFRP, Taylor JD, Taylor AFS, Khoo E, Majalap-Lee N, Helgason T, Johnson D (2018) Partitioning of soil phosphorus among arbuscular and ectomycorrhizal trees in tropical and subtropical forests. Ecol Lett 21:713–723. https://doi.org/10.1111/ele.12939

Lugli LF, Andersen KM, Aragão LE, Cordeiro AL, Cunha HF, Fuchslueger L, Rosa JS (2020) Multiple phosphorus acquisition strategies adopted by fine roots in low-fertility soils in central Amazonia. Plant Soil 450:49–63. https://doi.org/10.1007/s11104-019-03963-9

Lugli LF, Rosa JS, Andersen KM et al (2021) Rapid responses of root traits and productivity to phosphorus and cation additions in a tropical lowland forest in Amazonia. New Phytol 230:116–128. https://doi.org/10.1111/nph.17154

Lynch JP, Ho MD (2005) Rhizoeconomics: carbon costs of phosphorus acquisition. Plant Soil 269:45–56. https://doi.org/10.1007/s11104-004-1096-4

Malhi Y, Wright J (2004) Spatial patterns and recent trends in the climate of tropical rainforest regions. Phil Trans r Soc Lond b 359:311–329. https://doi.org/10.1098/rstb.2003.1433

Nasto MK, Osborne BB, Lekberg Y, Asner GP, Balzotti CS, Porder S, Taylor PG, Townsend AR, Cleveland CC (2017) Nutrient acquisition, soil phosphorus partitioning and competition among trees in a lowland tropical rain forest. New Phytol 214:1506–1517. https://doi.org/10.1111/nph.14494

Oliveira PHG, Gama-Rodrigues AC, Gama-Rodrigues EF, Sales MVS (2018) Litter and soil-related variation in functional group abundances in cacao agroforests using structural equation modeling. Ecol Indic 84:254–262. https://doi.org/10.1016/j.ecolind.2017.08.030

Pang J, Ruchi B, Zhao R, Bansal H, Bohhuon E, Lambers H, Ryan MH, Ranathunge K, Siddique KHM (2018) The carboxylate-releasing phosphorus- mobilizing strategy can be proxied by foliar manganese concentration in a large set of chickpea germplasm under low phosphorus supply. New Phytol 219:518–529. https://doi.org/10.1111/nph.15200

Postma JA, Dathe A, Lynch JP (2014) The optimal lateral root branching density for maize depends on nitrogen and phosphorus availability. Plant Physiol 166:590–602. https://doi.org/10.1104/pp.113.233916

Quesada CA, Lloyd J, Anderson LO, Fyllas NM, Schwarz M, Czimczik CI (2011) Soils of Amazonia with particular reference to the RAINFOR sites. Biogeosciences 8:1415–1440. https://doi.org/10.5194/bg-8-1415-2011

Raven JA, Lambers H, Smith SE, Westoby M (2018) Costs of acquiring phosphorus by vascular land plants: patterns and implications for plant coexistence. New Phytol 217:1420–1427. https://doi.org/10.1111/nph.14967

Reichert T, Rammig A, Fuchslueger L, Lugli LF, Quesada CA, Fleischer K (2022) Plant phosphorus-use and -acquisition strategies in Amazonia. New Phytol. https://doi.org/10.1111/nph.17985

Richardson AE, Barea JM, McNeill AM, Prigent-Combaret C (2009) Acquisition of phosphorus and nitrogen in the rhizosphere and plant growth promotion by microorganisms. Plant Soil 321:305–339. https://doi.org/10.1007/s11104-009-9895-2

Richardson AE, Simpson RJ (2011) Soil microorganisms mediating phosphorus availability update on microbial phosphorus. Plant Physiol 156:989–996. https://doi.org/10.1104/pp.111.175448

Rinaldi LCB, Aleixo S, Silva EC, Gama-Rodrigues AC, Gama-Rodrigues EF, Gonçalves JLM, Rocha JHT, Schripsema J (2021) $^{31}$P NMR spectroscopy and structural models of soil organic phosphorus under *Eucalyptus*. Nutr Cycl Agroecosyst 120:83–97. https://doi.org/10.1007/s10705-021-10139-4

Rubaek GH, Sibbesen E (1993) Resin extraction of labile, soil organic phosphorus. Eur J Soil Sci 44:467–478. https://doi.org/10.1111/j.1365-2389.1993.tb00469.x

Ryan MH, Tibbett M, Edmonds-Tibbett T, Suriyagoda LD, Lambers H, Cawthray GR, Pang J (2012) Carbon trading for phosphorus gain: the balance between rhizosphere carboxylates and arbuscular mycorrhizal symbiosis in plant phosphorus acquisition. Plant Cell Environ 35:2170–2180. https://doi.org/10.1111/j.1365-3040.2012.02547.x

Sales MVS, Gama-Rodrigues AC, Gama-Rodrigues EF (2017) Structural equation modeling for the estimation of interconnections between the P cycle and soil properties. Nutr Cycl Agroecosyst. https://doi.org/10.1007/s10705-017-9879-1

Smith SE, Jakobsen I, Gronlund M, Smith FA (2011) Roles of arbuscular mycorrhizas in plant phosphorus nutrition: interactions between pathways of phosphorus uptake in arbuscular mycorrhizal roots have important implications for understanding and manipulating plant phosphorus acquisition. Plant Physiol 156:1050–1057. https://doi.org/10.1104/pp.111.174581

Turner BL (2008) Soil organic phosphorus in tropical forests: an assessment of the NaOH–EDTA extraction procedure for quantitative analysis by solution $^{31}$P NMR spectroscopy. Eur J Soil Sci 9:453–466. https://doi.org/10.1111/j.1365-2389.2007.00994.x

Turner BL, Condron LM (2013) Pedogenesis, nutrient dynamics, and ecosystem development:the legacy of TW Walker and JK Syers. Plant Soil 367:1–10. https://doi.org/10.1007/s11104-013-1750-9

van der Heijden MG, Martin FM, Selosse MA, Sanders IR (2015) Mycorrhizal ecology and evolution: the past, the present, and the future. New Phytol 205:1406–1423. https://doi.org/10.1111/nph.13288

Vance CP, Uhde-Stone C, Allan DL (2003) Phosphorus acquisition and use: critical adaptations by plants for securing a nonrenewable resource. New Phytol 157:423–447. https://doi.org/10.1046/j.1469-8137.2003.00695.x

Viana TO, Gama-Rodrigues AC, Gama-Rodrigues EF, Aleixo S, Moreira RVS, Sales MVS, Marques JRB (2018) Phosphorus transformations in alfisols and ultisols under different land uses in the Atlantic Forest region of Brazil. Geoderma Reg 14:e00184. https://doi.org/10.1016/j.geodrs.2018.e00184

Walker TW, Syers JK (1976) The fate of phosphorus during pedogenesis. Geoderma 15:1–19. https://doi.org/10.1016/0016-7061(76)90066-5

Wen Z, Li H, Shen Q, Tang X, Xiong C, Li H, Pang J, Ryan MH, Lambers H, Shen J (2019) Tradeoffs among root morphology, exudation and mycorrhizal symbioses for phosphorus-acquisition strategies of 16 crop species. New Phytol 223:882–895. https://doi.org/10.1111/nph.15833

Wen Z, White PJ, Shen J, Lambers H (2022) Linking root exudation to belowground economic traits for resource acquisition. New Phytol 233:1620–1635. https://doi.org/10.1111/nph.17854

Yazdani M, Bahmanyar MA, Pirdashti H, Esmaili MA (2009) Effect of phosphate solubilization microorganisms (PSM) and plant growth promoting rhizobacteria (PGPR) on yield and yield components of corn (*Zea mays* L.). World Acad Sci Eng Technol 49:90–92. https://doi.org/10.5281/zenodo.1080014

Zhang L, Shi N, Fan J, Wang F, George TS, Feng G (2018) Arbuscular mycorrhizal fungi stimulate organic phosphate mobilization associated with changing bacterial community structure under field conditions. Environ Microbiol 20:2639–2651. https://doi.org/10.1111/1462-2920.14289